Mode of Action of Interleukin-6 on Mature Osteoclasts. Novel Interactions with Extracellular Ca^{2+} Sensing in the Regulation of Osteoclastic Bone Resorption

Olugbenga A. Adebanjo,* Baljit S. Moonga,* Tomoo Yamate,‡ Li Sun,* Cedric Minkin,§ Etsuko Abe,‡ and Mone Zaidi*

*Center for Osteoporosis and Skeletal Aging, Veterans Affairs Medical Center, and Department of Medicine, Medical College of Pennsylvania–Hahnemann School of Medicine, Philadelphia, Pennsylvania 19104; ‡Division of Endocrinology, University of Arkansas for Medical Sciences, Little Rock, Arkansas 72205; and §School of Dentistry, University of Southern California, Los Angeles, California 90089

Abstract. We describe a physiologically significant mechanism through which interleukin-6 (IL-6) and a rising ambient Ca^{2+} interact to regulate osteoclastic bone resorption. VOXEL-based confocal microscopy of nonpermeabilized osteoclasts incubated with anti–IL-6 receptor antibodies revealed intense, strictly peripheral plasma membrane fluorescence. IL-6 receptor expression in single osteoclasts was confirmed by in situ reverse transcriptase PCR histochemistry. IL-6 (5 ng/l to 10 μg/l), but not IL-11 (10 and 100 μg/l), reversed the inhibition of osteoclastic bone resorption induced by high extracellular Ca^{2+} (15 mM). The IL-6 effect was abrogated by excess soluble IL-6 receptor (500 μg/l). Additionally, IL-6 (5 pg/l to 10 μg/l) inhibited cytosolic Ca^{2+} signals triggered by high Ca^{2+} or Ni^{2+}. In separate experiments, osteoclasts incubated in 10 mM Ca^{2+} or on bone released more IL-6 than those in 1.25 mM Ca^{2+}. Furthermore, IL-6 mRNA histostaining was more intense in osteoclasts in 10 or 20 mM Ca^{2+} than cells in 1.25 mM Ca^{2+}. Similarly, IL-6 receptor mRNA histostaining was increased in osteoclasts incubated in 5 or 10 mM Ca^{2+}. Thus, while high Ca^{2+} enhances IL-6 secretion, the released IL-6 attenuates Ca^{2+} sensing and reverses inhibition of resorption by Ca^{2+}. Such an autocrine–paracrine loop may sustain osteoclastic activity in the face of an inhibitory Ca^{2+} level generated locally during resorption.

Key words: IL-6 • Ca^{2+} sensing • Ca^{2+} receptor • osteoporosis • ryanodine receptor

Interleukin-6 (IL-6)[1] has a role in bodily functions as critical as hematopoiesis, immune regulation, neoplastic transformation, bone metabolism, reproduction, arthritis, and aging. The cytokine interacts with an 80-kD glycoprotein receptor that signals through a ubiquitous molecule, gp130 (Manolagas and Jilka, 1995). Like certain related cytokines, IL-6 is critical to the enhanced osteoclastogenesis and bone resorption that follows ovariectomy (Jilka et al., 1992; Tamura et al., 1993; Manolagas and Jilka, 1995). In addition, it is known that, by interacting with the NFκB site, estrogen regulates IL-6 gene transcription directly (Kurebayashi et al., 1997). IL-6 has also been shown to prevent osteoclast apoptosis (Hughes et al., 1995). Finally, IL-6 promotes a maturer osteoblast phenotype through the Janus signal transducer and activator of transcription (STAT) pathway (Bellido et al., 1997).

Osteoclast-like cells from giant cell tumors of bone can themselves synthesize and secrete IL-6 (Ohsaki et al., 1992). In addition, IL-6 stimulates pit formation by rat and human osteoclasts (Ishimi et al., 1990; Ohsaki et al., 1992). It has even been speculated that parathyroid hormone acts through the rapid stimulation of osteoblastic IL-6 gene expression, whereby the released cytokine stimulates resorption (Greenfield et al., 1996). Furthermore, the osteolysis characteristic of multiple myeloma, Paget's disease of bone, and the rare Gorham-Stout's disease appears to result not only from IL-6 stimulation of osteoclastogenesis but also from an increase in the activity of existing osteoclasts (Roodman et al., 1992; Delvin et al., 1996). Thus,

Drs. Yamate and Sun are equal contributors to the work.

Address all correspondence to Mone Zaidi, M.D., Ph.D., Geriatrics and Extended Care (11G), VA Medical Center, Woodlands and University Avenues, Philadelphia, PA 19104. Tel.: (215) 823-4400. Fax: (215) 823-6715. E-mail: zaidim@auhs.edu

1. *Abbreviations used in this paper*: ANOVA, analysis of variance; CSI, corrected staining intensity; DEPC, diethyl pyrocarbonate; DIG, digoxigenin; GA3PD, glyceraldehyde 3-phosphate dehydrogenase; IL-6, interleukin-6; IL-6R, IL-6 receptor; rhIL-6, human recombinant IL-6; RT-PCR, reverse transcriptase PCR; TRAP, tartrate-resistant acid phosphatase.

while a direct effect of IL-6 on mature osteoclasts has appeared plausible, molecular insights have largely been lacking.

Mature osteoclasts are inhibited by the calcitonin, prostaglandins, nitric oxide, and calcium ions (Ca^{2+}) (Malgaroli et al., 1989; Zaidi et al., 1989, 1994; MacIntyre et al., 1991; Adebanjo et al., 1994). During resorption, Ca^{2+} levels rise to millimolar levels within the resorptive hemivacuole (Silver et al., 1988). This rising Ca^{2+} concentration is "sensed" by the osteoclast through a surface Ca^{2+} receptor that, we believe, is a functional component of the surface-expressed ryanodine receptor (Zaidi et al., 1995). Ca^{2+} receptor activation results in both transmembrane Ca^{2+} influx and intracellular Ca^{2+} release (Shankar et al., 1992; Zaidi et al., 1993*c*). The resulting cytosolic Ca^{2+} increase inhibits osteoclast attachment, proteolytic enzyme release, and bone resorption (Malgaroli et al., 1989; Moonga et al., 1990; Zaidi et al., 1993*b*). There is also a direct and highly significant correlation between cytosolic Ca^{2+} and resorption inhibition (Zaidi et al., 1989, 1990; Moonga et al., 1991).

In the present study, we have attempted to explore potential interactions between extracellular Ca^{2+} and IL-6 in mature active osteoclasts. We find that (*a*) osteoclasts express IL-6 and IL-6 receptor (IL-6R); (*b*) IL-6 reverses Ca^{2+}-induced resorption inhibition and attenuates Ca^{2+} sensing; and (*c*) high Ca^{2+} enhances IL-6 and IL-6R gene expression and IL-6 secretion. We therefore hypothesize that IL-6 production increases when an osteoclast becomes exposed to an otherwise inhibitory Ca^{2+} level during resorption. The IL-6 so produced then sustains resorption, at least in part, by attenuating extracellular Ca^{2+} sensing.

Materials and Methods

Osteoclast Culture

Osteoclasts were obtained by curetting neonatal rat (24 to 48 h old, Wistar) long bones into 1 ml Hepes-buffered medium 199 containing Hanks' salts (M199-H) (GIBCO-BRL, Grand Island, NY) and heat-inactivated FBS (5% vol/vol; Sigma Chemical Co., St. Louis, MO). The resulting suspension was dispersed onto prewetted devitalized cortical bone slices (4 × 4 mm) or 22-mm, 0-grade glass coverslips (ICN Biomedicals, Inc., Aurora, OH). Osteoclasts readily attached to the respective substrate within 30 min (37°C), and nonadherent cells were removed by rinsing (Zaidi et al., 1992).

Monoclonal Anti–IL-6R Antibodies

We used two highly specific anti–IL-6R monoclonal antibodies, namely MT-18 (kindly provided by Dr. T. Taga, Osaka University, Osaka, Japan) and 15A7 (BioSource International, Inc., Camarillo, CA). MT-18 was raised to human IL-6R that was overexpressed in IL-6R–negative murine T cell line, CTLL-2 (Hirata et al., 1989). The antibody detects the IL-6R specifically by immunodetection methods, cell growth studies, and ^{125}I–IL-6 binding assays (Hirata et al., 1989; Taga et al., 1989; Ohsaki et al., 1992; May et al., 1993; Narazaki et al., 1993). 15A7 is an affinity-purified monoclonal antibody raised to the murine IL-6R expressed in OKT4 plasmacytoma cells. It recognizes mouse, human, and rat IL-6R (Vink et al., 1990). Note that at the protein level, human IL-6R (X12830) is ~55% homologous to rat (M58587) or mouse (X51975) IL-6R; the latter two receptors bear ~95% homology (GeneBank CDS, PDB and Swissprot Databanks, Blast Search Software).

Immunocytochemistry, Confocal Microscopy, and VOXEL Analysis

Osteoclasts were incubated with normal goat serum (in 10 mM PBS, 1:10, pH 7.4) in multiwell dishes (15 min) and washed with HBSS (GIBCO-BRL). The cells were either incubated with no antibody, nonimmune mouse serum, an anti–ryanodine receptor antibody, Ab^{34} (all controls), or with MT-18 or 15A7 (in M199-H, 1:100 vol/vol). Notably, Ab^{34}, raised against a cytosolic ryanodine receptor epitope, does not stain nonpermeabilized osteoclasts (Zaidi et al., 1995). In the same experiment, IL-6R–negative osteoblastic MBA13.2 cells (Zipori et al., 1985) were also incubated with the same antibodies. Additionally, a set of coverslips were incubated simultaneously with soluble (truncated) human recombinant (rh) IL-6R (~38 kD; R & D Systems, Minneapolis, MN), together with MT-18. After 1 h of incubation, coverslips were rinsed gently with HBSS, drained, reincubated with goat anti–mouse FITC (Sigma Chemical Co.; in HBSS, 1:100, 1 h) (FITC: λ_{ex} = 495 nm, λ_{em} = 525 nm), washed gently, and drained.

The number of fluorescent osteoclasts was first determined in a laser confocal scanning microscope (Leica, Inc., Deerfield, IL). To localize staining to the osteoclast membrane, 1-μm-thick optical sections were obtained in the cell's coronal plane in selected experiments (Zaidi et al., 1995). Each optical plane was then visualized by VOXEL (volume element) image analysis, which allowed a final three-dimensional reconstruction of the cell image (VoxelView; Vital Images Inc., Fairfield, IA). Finally, trypan blue (1 mM, 961 D; Sigma Chemical Co.) was applied to exclude significant membrane damage that could potentially allow antibody access into the cytosol.

Molecular Cytoimaging by In Situ Reverse Transcriptase PCR

Recently, the in situ reverse transcriptase (RT)-PCR method has been applied successfully to study IL-6 and IL-6R expression in osteoblasts and bone marrow stromal cells (Lin et al., 1997). We have now examined IL-6, IL-6R, and glyceraldehyde 3-phosphate dehydrogenase (GA3PD) expression in mature osteoclasts in response to changes in extracellular Ca^{2+}. Primer sequences were as follows (Lin et al., 1997): IL-6 J03783 5′-primer 49–73 ATGAAGTTCCTCTCTGCAAGAGACT, 3′-primer 686–663 CACTAGGTTTGCCGAGTAGATCTC; IL-6R X51975 5′-primer 383–404 TGTCAACGCCATCTGTGAGTGG, 3′-primer 1046–1025 ACTTTCGTACTGATCCTCGTGG; and GA3PD M32599 5′-primer 51–76 TGAAGGTCGGTGTGAACGGATTTGGC, 3′-primer 1033–1010 CATGTAGGCCATGAGGTCCACCAC.

Osteoclasts were incubated on glass coverslips (22 mm, 0 grade) in medium 199 with Earle's salts (6.6 mM Na_2CO_3, M199-E; 6 h, 37°C, 5% humidified CO_2, pH 7.4) in the presence of different Ca^{2+} concentrations (1.25, 5, 10, or 20 mM). They were washed with M199-E, fixed with paraformaldehyde (4%, vol/vol) in PBS (20 min, 4°C), and washed twice with cold PBS. The fixed cells were treated subsequently with 0.2 N HCl for an additional 20 min (20°C) and washed with diethyl pyrocarbonate (DEPC)-water (Sigma Chemical Co.). The cells were then treated with proteinase-K (5 mg/l in 10 mM Tris-HCl, pH 8.0; 15 min, 37°C) and cold paraformaldehyde (4% vol/vol; 30 min, 4°C). They were next dehydrated by immersing coverslips, for 1 min each time in aqueous ethanol solutions 70, 80, 90, and 100% (vol/vol) and were subsequently air-dried. Osteoclasts were then incubated overnight (37°C) with RNase-free, DNase I (1,500 U/ml; Boehringer Mannheim Corp., Indianapolis, IN) to remove genomic DNA.

DNase I was washed out with DEPC-water and heat-inactivated (90°C) for 10 min. First-strand cDNA was next synthesized by incubating coverslips with RT mixture (50 μl) composed of 1 mM dNTP, 0.01 M DTT, 400 nM gene-specific antisense (3′-end) primer (above), DEPC-water, and 14 U/ml Superscript RT II (GIBCO-BRL) (42°C, 60 min). For PCR amplification of the synthesized DNA, the samples were treated separately with PCR mixture (50 μl) composed of 0.2 mM dNTP, PCR buffer, 2.5 mM $MgCl_2$, 0.1 U/μl Taq polymerase, 400 nM sense (5′-end) and antisense (3′-end) primers, 10 μM digoxigenin (DIG)-labeled-11-dUTP (Boehringer Mannheim Corp.), and DEPC-water. Each sample was then covered gently with an AmpliCover disc ensuring the absence of air bubbles. The GeneAmp In situ PCR System 1000 (Perkin Elmer Corp., Norwalk, CT) was programmed as follows: 4-min soak (94°C) followed by 40 cycles each of 94°C/1 min, 65°C/2 min, and 72°C/3 min.

Incorporated DIG-11-dUTP in the PCR product was detected by an alkaline phosphatase–conjugated anti-DIG antiserum and alkaline phosphatase substrates, 4-nitroblue tetrazolium chloride and 5-bromo-4-chloro-3-indoyl-phosphate, using a DIG Nucleic Acid Detection Kit (Boehringer Mannheim Corp.) as per manufacturer's protocol. To illustrate successful removal of genomic DNA by DNase treatment, we excluded the specific primers. We also ran controls that omitted the DNase step (method validated as described; Lin et al., 1997).

The purple-brown staining in randomly selected cells (up to 25 cells per variable) was quantitated by image analysis (SAMBA International Inc., Chantilly, VA). In each experiment, the background staining intensity was assessed from cells that were not incubated with primer. Staining intensity was expressed as arbitary units per unit cell area (corrected staining intensity [CSI]). The mean CSI was compared for statistical differences by analysis of variance (ANOVA) and Bonferroni's correction for inequality. Most osteoclasts were well spread; the very few cells that were retracted were excluded from the analysis. Although this may somewhat bias the results, it would prevent critical false-positive enhancements in staining resulting from cytoplasmic condensation. Thus, although done to the best of our ability, in situ RT-PCR quantitation is inherently fraught with interpretational difficulties, and to address these issues, we studied the expression of the housekeeping gene, GA3PD.

Bone Resorption Assay

Bone resorption was measured using the pit assay of Boyde et al. (1984) and Chambers et al. (1984), which was later modified by Dempster et al. (1987). Once osteoclasts had sedimented (see above), the bone slices were transferred to a multiwell dish containing medium 199 (M199-E) and 10% (vol/vol) FBS. The following sets of experiments were performed: set A, 1.25 mM Ca^{2+} (control) or 15 mM Ca^{2+} with/without different concentrations of rhIL-6 (5 ng/l, 0.5 μg/l, and 10 μg/l) (R & D Systems); set B, 1.25 mM Ca^{2+} (control) or 15 mM Ca^{2+} with/without different concentrations of rhIL-11 (10 and 100 μg/l) (R & D Systems); and set C, 1.25 mM Ca^{2+} (control) or 15 mM Ca^{2+} with IL-6 (5 ng/l) in the presence or absence of the soluble rhIL-6R (500 μg/l). The slices were then incubated for 24 h in humidified CO_2 (5%) (pH = 6.9, maximal resorptive activity).

After incubation, the slices were fixed with glutaraldehyde (10%, vol/vol) and stained for tartrate-resistant acid phosphatase (TRAP) using a kit (Kit 386A; Sigma Chemical Co.). The number of osteoclasts with two or more nuclei was determined on each slice using a light microscope (Olympus, Tokyo, Japan). The cells were removed by treating the slices with NaOCl (5 min), and the slices were rinsed with distilled water followed by acetone and then dried. They were stained with toluidine blue (1%, vol/vol in 1%, wt/vol borate, 5 min), and the resorption pits were counted by light microscopy. Note that each experiment was performed with osteoclasts obtained from three animals with five or six replicate bone slices per treatment, and each experiment was repeated between three and five times. The number of pits per bone slice was expressed as a mean ± SEM. ANOVA with Bonferroni's correction for inequality was used to analyze the effect of treatment (significance at $P < 0.05$).

Microspectrofluorimetric Measurements of Cytosolic Ca^{2+}

Coverslips containing freshly isolated osteoclasts were incubated (30 min, 37°C) with 10 μM fura-2/AM (Molecular Probes, Eugene, OR) in serum-free medium. They were then washed in M199-H and transferred to a Perspex bath on the microspectrofluorimeter stage (model Diaphot; Nikon, Telford, UK). The cells were then exposed to prewarmed M199-H containing $CaCl_2$ (10 mM) or $NiCl_2$ (5 mM). In different experiments, osteoclasts were first conditioned for 3 or 4 min with IL-6 (5 pg/l to 10 μg/l) or IL-11 (100 μg/l). The cells were then exposed alternatively to excitation wavelengths of 340 or 380 nm every second. For recording the emitted fluorescence, a single osteoclast was selected by narrowing an optical diaphragm to approximate the cell's boundary. The cell was then removed, and a background count was obtained for 10 s. The average background fluorescence (counts per second) was then subtracted automatically from subsequent counts obtained from the selected cell. This emitted fluorescence was filtered at 510 nm, directed to a photomultiplier tube (model PM28B; Thorn EMI, London, UK), and counted by a dual photon counter (Newcastle Photometrics, Newcastle, UK). This gave a ratio of emitted intensities due to excitation at 340 and 380 nm, F_{340}/F_{380}. Fura-2 was calibrated by deriving values for R_{min}, F_{max}, R_{max}, and F_{min} that were substituted into the following equation: $[Ca^{2+}] = K_d \times [(R - R_{min})/(R_{max} - R)] \times [(F_{max}/F_{min})]$ (K_d = 224 nM at 20°C, 0.1 M, and pH 6.85) (Shankar et al., 1992).

Statistical comparisons between basal and peak cytosolic Ca^{2+} for the Ni^{2+}-induced cytosolic Ca^{2+} changes caused by each IL-6 concentration were made using the paired Student's *t* test. Mean changes (Δ) in the peak cytosolic Ca^{2+} level were calculated by subtracting the peak cytosolic Ca^{2+} level from basal. At the respective IL-6 concentrations, these were compared against control (cation alone) by ANOVA and Bonferroni's correction for inequality. Finally, the rate of rise of cytosolic Ca^{2+} was compared by linear regression analysis.

Supernatant IL-6 Measurements by ELISA

Osteoclasts were dispersed onto either glass coverslips or cortical bone slices (above). They were then bathed in a multiwell dish containing 500 μl M199-E and FBS (10%, vol/vol) for up to 16 h. At each time point, notably at 0.5, 1.5, 3.5, 7.5, 15.5, and 33 h, the entire supernatant was removed and replaced by fresh medium. Comparisons were made between three treatment variables: 1.25 mM Ca^{2+} on glass, 10 mM Ca^{2+} on glass, and 1.25 mM Ca^{2+} on bone.

IL-6 was measured using an ELISA kit (Kit M6000; R & D Systems). In brief, 96-well plates coated with mouse IL-6 polyclonal antiserum were used to accommodate 50 μl diluent (buffered protein) and 50 μl standard, control, or sample. After incubation (20°C, 2 h), the wells were aspirated, washed repeatedly, and loaded with 100 μl horseradish peroxidase–conjugated anti–IL-6 antibody. After a further 2-h incubation (20°C), 100 μl substrate solution containing H_2O_2 and tetramethylbenzidine was added to each well. Finally, a further incubation (30 min) was followed by the addition of 100 μl dilute HCl to stop the reaction. The optical density of each sample was recorded at 450 nm on a microplate reader (Bio-Rad Laboratories, Hercules, CA). Immunoreactive IL-6 was estimated from the standard curve in triplicate experiments. Precision and accuracy were assessed as per kit instructions. The accumulation and calculated rate of IL-6 release were represented as means ± SEM, and comparisons were made using ANOVA with Bonferroni's correction for inequality ($P < 0.05$).

Results

Confocal Microscopic Localization of IL-6 Receptors to the Osteoclast Plasma Membrane

Fig. 1, *a* and *c*, shows confocal microscopic images of osteoclasts stained with the anti–IL-6R antibodies, MT-18 and 15A7, respectively. The intense peripheral staining was distinctly reminiscent of a plasma membrane pattern. Notably, IL-6R–negative MBA13.2 cells did not stain with either MT-18 (Fig. 1 *d*) or 15A7 (not shown). Fig. 1, *e–g*, shows VOXEL (volume element) imaging of optical sections taken in the cell's coronal (Fig. 1 *e*) or sagittal (Fig. 1 *f*) planes. A three-dimensional VOXEL whole-cell image (Fig. 1 *g*) again confirmed a cell surface localization of the MT-18 staining. Every one of the ~100 osteoclasts examined in different experiments stained with both MT-18 and 15A7. All cells were negative for trypan blue.

Control experiments to test specificity of the antibody staining were performed by (*a*) not including antibodies MT-18 and 15A7, (*b*) using nonimmune mouse serum instead of the antibodies, (*c*) using an anti–ryanodine receptor antibody, Ab^{34}, and (*d*) including excess soluble rhIL-6R (500 μg/l) before and during incubation with the antibodies. Note that because the soluble rhIL-6R lacks a transmembrane region, it should not normally incorporate into the plasma membrane but should bind both MT-18 and 15A7. It should therefore displace the respective antibodies from their binding sites on the osteoclast. MT-18 staining intensity was reduced to a very faint glow, seen in Fig. 1 *b*, upon incubation with soluble rhIL-6R. Furthermore, the fact that osteoclasts did not stain with the Ab^{34}, nonimmune mouse serum, or when no antibody was added (not shown) provided further controls for specificity. Note that Ab^{34} is directed to a cytosolic ryanodine receptor epitope and does not stain the surface of nonpermeabilized osteoclasts (Zaidi et al., 1995).

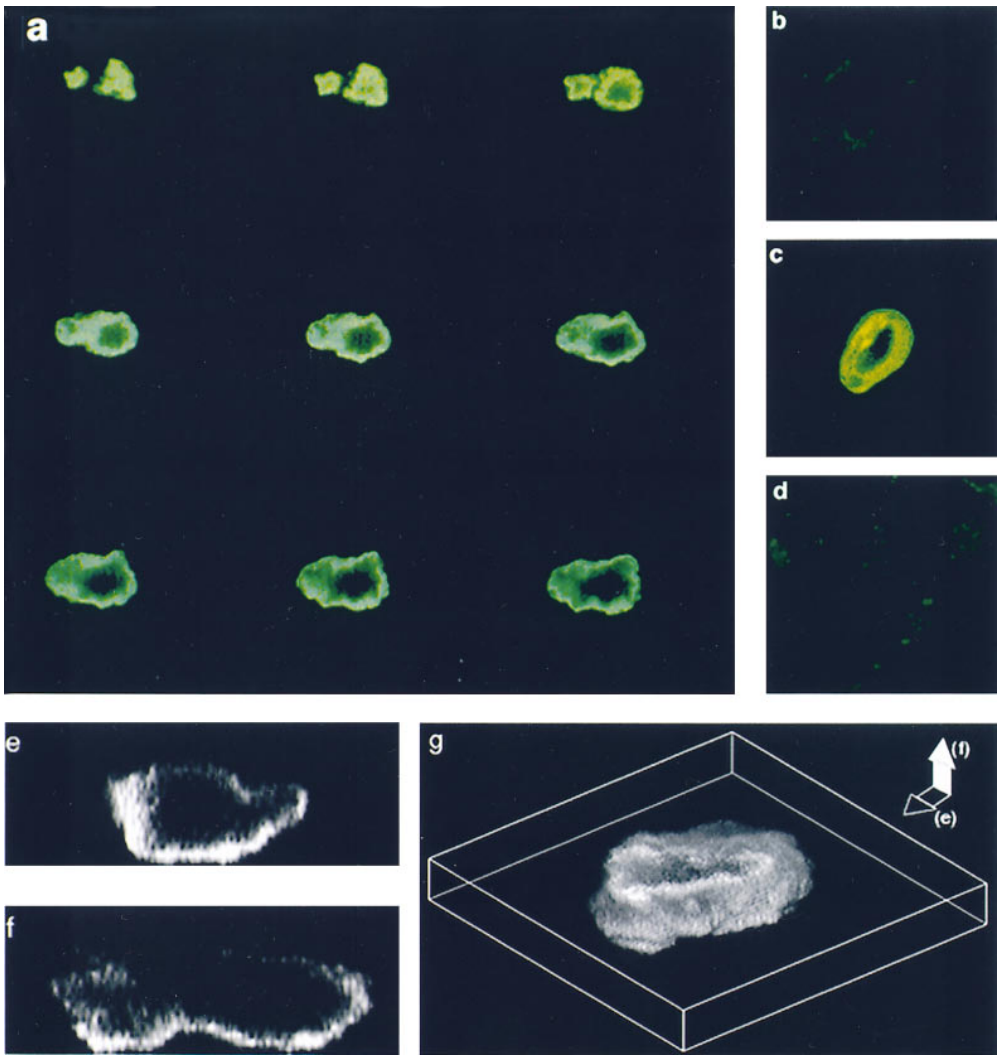

Figure 1. Confocal microscopic localization of the IL-6R on rat osteoclast plasma membrane. (*a* and *c*) Intense peripheral immunofluorescent staining of osteoclasts with two highly specific anti–IL-6R monoclonal antibodies, MT-18 (*a*; serial sections in coronal plane, 1 μm thick) and 15A7 (*c*; single coronal section). Note that osteoclasts incubated with no antiserum, nonimmune mouse serum, or an irrelevant antibody (Ab^{34}) did not stain (not shown). (*b*) Very faint staining of an osteoclast with MT-18 coincubated with soluble rhIL-6R (500 μg/l); this confirms IL-6R specificity of the antibody. (*d*) Lack of appreciable staining of IL-6R–negative MBA13.2 cells incubated with antibody, MT-18. For details on confocal microscopy, see Materials and Methods. (*e* and *f*) VOXEL (volume element) imaging of osteoclasts stained with the anti–IL-6R antibody, MT-18. This method allows three-dimensional optical sectioning in both the coronal (*e*) and sagittal (*f*) planes of the cell. Staining is typically localized to the cell's periphery with a sparing of the central cytoplasmic and nuclear areas. (*g*) A three-dimensional reconstruction of membrane staining from the coronal and sagittal sections.

Effect of IL-6 on the Resorptive Activity of Mature Rat Osteoclasts

The function of the expressed osteoclast IL-6R was next assessed in bone resorption assays. We confirmed that Ca^{2+} inhibited pit number per slice significantly ($P = 0.007$; $n = 5$ slices per experiment) in all five experiments (Fig. 2 *a*). IL-6 itself, at concentrations of 5 ng/l, 0.5 μg/l, and 10 μg/l, did not significantly enhance resorption ($P = 0.205$, 0.126, and 0.48, respectively; $n = 10$ slices/concentration, up to five experiments). However, at all three concentrations, IL-6 reversed the resorption inhibition induced by Ca^{2+} (Fig. 2 *a*). Thus, when IL-6 was applied together with Ca^{2+}, the pit number per slice was significantly different from that on the Ca^{2+}-treated slices ($P = 0.002$, 0.026, and 0.05, respectively, for the three IL-6 concentrations; $n = 10$) (Fig. 2 *a*). The number of TRAP-positive multinucleated cells did not change with any of the above treatments.

We used the related cytokine, IL-11, at two concentrations (10 and 100 μg/l). Note that IL-11 and IL-6 are known to trigger intracellular signaling by binding to the same transducer, gp130. However, IL-11, even at a relatively high concentration, failed to reverse Ca^{2+}-induced resorption inhibition (Fig. 2 *b*). Thus, the significant inhibition of resorption seen with Ca^{2+} ($P < 0.001$, $n = 5$ slices) still persisted despite IL-11 application ($P < 0.001$, for both concentrations compared with control; $n = 5$ slices) (Fig. 2 *b*).

Finally, we used the soluble rhIL-6R in competition experiments. As explained above, soluble IL-6R is expected to displace IL-6 from its surface-binding sites. Likewise, we found that soluble rhIL-6R (500 μg/l) reversed the effect of IL-6 (5 ng/l) in attenuating the resorption inhibition induced by 15 mM Ca^{2+} (Fig. 2 *c*). Thus, there was no significant difference ($P = 0.733$; $n = 5$ slices) between resorption by osteoclasts treated with Ca^{2+} alone and those treated with Ca^{2+}, IL-6, and soluble rhIL-6R. As expected, soluble rhIL-6R did not itself significantly affect bone re-

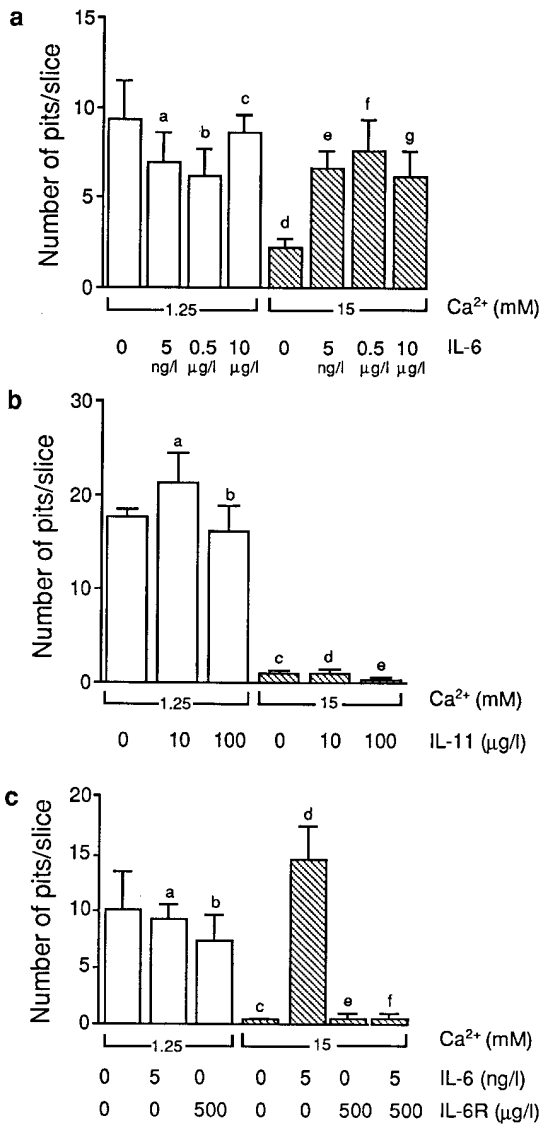

Figure 2. (*a*) Bone resorption by isolated rat osteoclasts, expressed as the mean pit number per bone slice (±SEM), in the presence of different concentrations of IL-6 and $CaCl_2$ (Ca^{2+}), as shown. Statistics by ANOVA with Bonferroni's correction for inequality. Compared with control: $^{a}P = 0.205$, $^{b}P = 0.126$, $^{c}P = 0.418$, and $^{d}P = 0.007$; compared with 15 mM Ca^{2+}: $^{e}P = 0.002$, $^{f}P = 0.026$, and $^{g}P = 0.05$. (*b*) Bone resorption by isolated rat osteoclasts, expressed as the mean pit number per bone slice (±SEM), in the presence of different concentrations of IL-11 and $CaCl_2$ (Ca^{2+}), as shown. Statistics by ANOVA with Bonferroni's correction for inequality. Compared with control: $^{a}P = 0.621$, $^{b}P = 0.317$, and $^{c-e}P < 0.001$. (*c*) Bone resorption by isolated rat osteoclasts, expressed as the mean pit number per bone slice (±SEM) in the presence of different concentrations of $CaCl_2$ (Ca^{2+}), IL-6, and/or the soluble rhIL-6R, as shown. Statistics by ANOVA with Bonferroni's correction for inequality. Compared with control: $^{a}P = 0.847$, $^{b}P = 0.536$, $^{c,e,f}P < 0.001$, and $^{d}P = 0.675$.

sorption (cf., control, $P = 0.536$, $n = 5$ slices), while IL-6 alone abolished the Ca^{2+} effect (cf., Ca^{2+} alone, $P = 0.001$, $n = 5$ slices) (Fig. 2 *c*). Taken together, the results suggest strongly that the attenuation of Ca^{2+}-induced resorption inhibition is highly specific to IL-6 and appears not to be shared by related cytokines, such as IL-11.

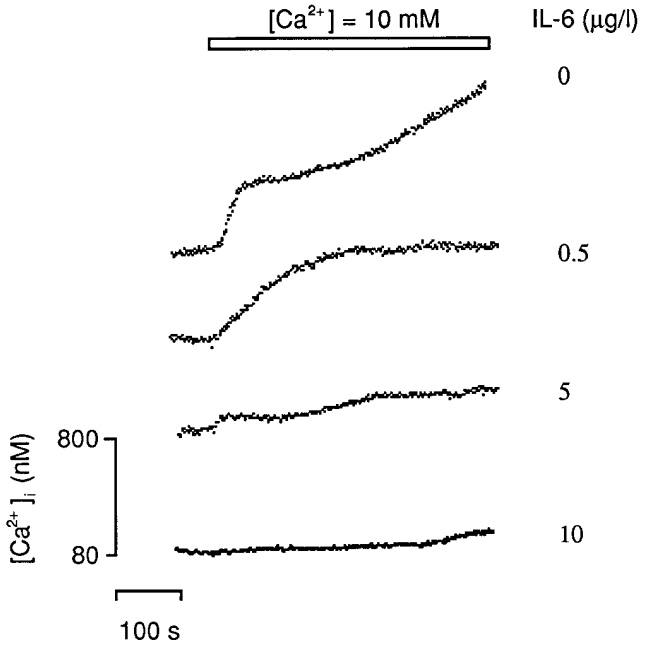

Figure 3. Representative traces showing the effect of IL-6 on cytosolic Ca^{2+} levels elicited in fura-2–loaded rat osteoclasts in response to 10 mM Ca^{2+} applied extracellularly with either vehicle or 0.5, 5, or 10 µg/l IL-6 (n = 4–6 cells for each variable). For statistical analysis, see Table I.

Effect of IL-6 on Extracellular Ca^{2+} (Cation) Sensing by Isolated Osteoclasts

We measured cytosolic Ca^{2+} levels in fura-2–loaded osteoclasts that were exposed to IL-6 (5 ng/l, 0.5 µg/l, 5 µg/l, or 10 µg/l) and 10 mM Ca^{2+}. In separate experiments, osteoclasts were preincubated for between 3 and 4 min, with a range of IL-6 concentrations (5 pg/l to 10 µg/l) or with 100 µg/l IL-11, and then exposed to 5 mM Ni^{2+}. Of note is that activation of the Ca^{2+} receptor by Ni^{2+} triggers intracellular Ca^{2+} release selectively (Caputo, 1981; Shankar et al., 1992). In contrast, an elevated extracellular Ca^{2+} triggers both Ca^{2+} release and Ca^{2+} influx, resulting in a rapid rise of cytosolic Ca^{2+} followed by its sustained elevation (Zaidi et al., 1993*a*).

Table I.

Treatments	Δ_p	Δ_s	τ_s
	nM	*nM*	*nM/s*
Ca^{2+} alone	25.6 ± 6.93	652 ± 19.2	0.54 ± 0.02
Ca^{2+} + IL-6 (5ng/l)	19.8 ± 4.91	44.7 ± 8.36*	0.39 ± 0.07
Ca^{2+} + IL-6 (0.5 µg/l)	0.05*	12.5 ± 3.10*	0.23 ± 0.11
Ca^{2+} + IL-6 (5 µg/l)	0.6*	5.71 ± 1.55*	0.17 ± 0.05‡
Ca^{2+} + IL-6 (10 µg/l)	0	28.3 ± 24.5*	0.15 ± 0.01‡

The effect of IL-6 on the primary and secondary cytosolic Ca^{2+} responses elicited by 10 mM Ca^{2+} applied extracellularly. The mean change (Δ) (±SEM) cytosolic Ca^{2+} was calculated from the difference between basal and either peak (Δ_p at 100 s, for the primary response) or plateau (Δ_s at 500 s, for the secondary response). The rate of change of cytosolic Ca^{2+} (τ_s) was calculated from the slope of the slowly rising phase of the secondary response. Significant differences: Δ_p and Δ_s compared with control (Ca^{2+} alone), $^{*}P < 0.001$. The τ_s values for 5 and 10 µg/l IL-6 were significantly ($^{‡}P < 0.02$) different from control (Ca^{2+} alone) (n = 4–6 cells).

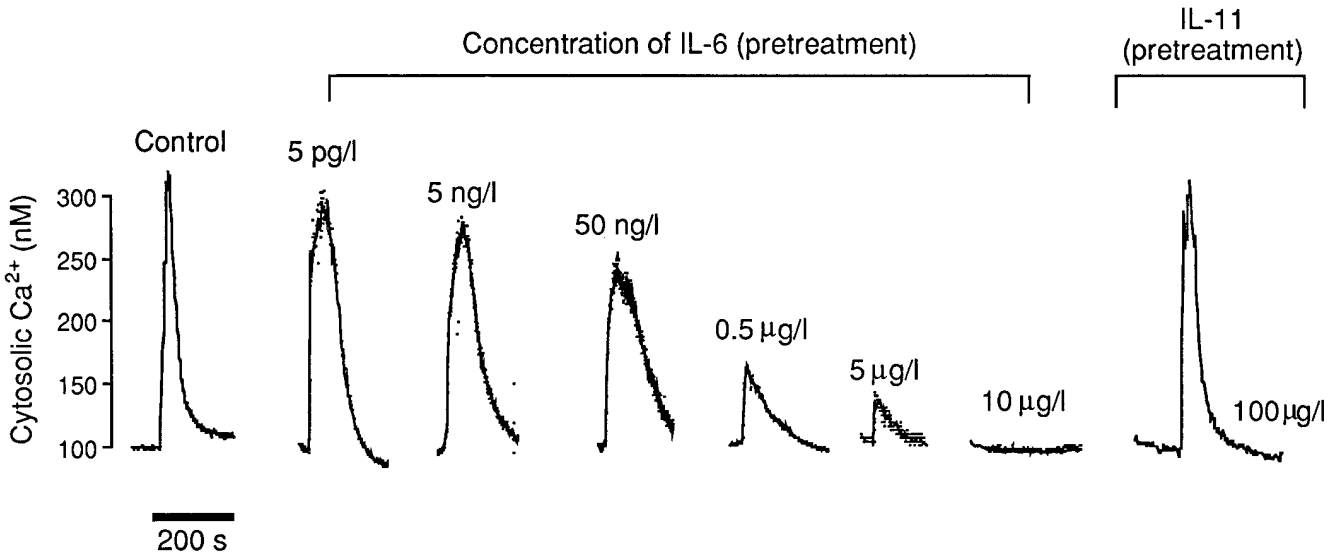

Figure 4. Representative traces showing the effect of preincubation with either IL-6 (5 pg/l to 10 μg/l) or IL-11 (100 μg/l) on cytosolic Ca^{2+} levels in fura-2–loaded rat osteoclasts elicited in response to the application of 5 mM Ni^{2+} extracellularly (n = 4–6 cells for each variable). For statistical analysis, see Table II.

We found that exposure of osteoclasts to IL-6 (5 ng/l, 0.5 μg/l, 5 μg/l, and 10 μg/l) resulted in no change in cytosolic Ca^{2+} for up to 10 min. As expected, application of 10 mM Ca^{2+} alone triggered a rapid, approximately fivefold elevation in cytosolic Ca^{2+} resulting from Ca^{2+} release ("primary" response); this was followed by a slow Ca^{2+} influx ("secondary" response) (Fig. 3). IL-6 attenuated (*a*) the primary Ca^{2+}-induced Ca^{2+} release response (Δ_p, Table I) at 0.5 μg/l and above, and (*b*) the secondary, more prolonged Ca^{2+} influx response (Δ_s, Table I) at a lower concentration (5 ng/l). Note that complete reversal of Ca^{2+}-induced resorption inhibition occurs at IL-6 concentrations as low as 5 ng/l (cf., Fig. 2 *a*).

We next attempted to characterize further the IL-6 effect on Ca^{2+} (cation) sensing by using Ni^{2+}. Application of Ni^{2+}, at a concentration of 5 mM, resulted (as previously) in a rapid rise of cytosolic Ca^{2+} to a peak within 50 s, followed by an exponential decay to near-basal levels within 150 s. Preincubation of osteoclasts with IL-6 (between 5 pg/l and 10 μg/l) resulted in a progressively diminishing Ni^{2+}-induced cytosolic Ca^{2+} signal; this attenuation was significant at 50 ng/l IL-6 (P = 0.035), and complete abrogation occurred at 10 μg/l (Fig. 4, Table II). Table II presents a comparison of the magnitudes of the Ni^{2+}-induced cytosolic Ca^{2+} response at each IL-6 concentration. Note that the related cytokine, IL-11, used at 100 μg/l did not attenuate Ni^{2+}-induced cytosolic Ca^{2+} elevation, suggesting that this action was specific to IL-6. Taken together, the results with Ca^{2+} and Ni^{2+} indicate that extracellular Ca^{2+} (cation) sensing by the osteoclast is inhibited strongly by IL-6 but not by the related cytokine, IL-11.

Effect of Ca^{2+} on IL-6 Production in Osteoclast Cultures

Osteoclasts were incubated in M199-E either on glass coverslips (1.25 or 10 mM Ca^{2+}) or on bone slices (1.25 mM Ca^{2+}). The supernatant was decanted at 0.5, 1.5, 3.5, 7.5, 15.5, and 33 h, and an equal volume of fresh medium was replaced. Estimates of the cumulative IL-6 concentration and release rate were obtained for each time point. It should be noted that other contaminating cells in our cultures might contribute to the measured IL-6. Fig. 5 *a* shows that for all three treatment variables, the mean cu-

Table II.

Treatments	Pretreatment	Peak	Posttreatment	Δ
Ni^{2+} 5 mM alone	117 ± 3.87	636 ± 50.7*	144 ± 8.25	519 ± 40.8
IL-11 (100 μg/l) then Ni^{2+}	72.0 ± 10.5	545 ± 245	57.9 ± 9.87	473 ± 255‡
IL-6 (5 pg/l) then Ni^{2+}	139 ± 26.3	618 ± 126*	184 ± 78.3	477 ± 120§
IL-6 (5 ng/l) then Ni^{2+}	123 ± 14.4	552 ± 135*	128 ± 23.0	429 ± 131‖
IL-6 (50 ng/l) then Ni^{2+}	87.9 ± 15.4	268 ± 124	127 ± 30.0	180 ± 111¶
IL-6 (0.5 μg/l) then Ni^{2+}	82.5 ± 6.0	257 ± 30.9*	82.5 ± 6.0	176 ± 24.8**
IL-6 (5 μg/l) then Ni^{2+}	96.3 ± 28.0	161 ± 28.9	88.9 ± 16.4	64.2 ± 39.6**
IL-6 (10 μg/l) then Ni^{2+}	122 ± 27.8	138 ± 36.0	105 ± 19.4	16.3 ± 12.6**

The effect of IL-6 and IL-11 on the magnitude of cytosolic Ca^{2+} transients elicited in response to the application of 5 mM Ni^{2+}. The table displays values of cytosolic Ca^{2+} (nM, ±SEM, n = 4–6 cells) computed before (*Pretreatment*), during (*Peak*), and after (*Posttreatment*) application of 5 mM Ni^{2+}. The change (Δ) in cytosolic Ca^{2+} (±SEM) is also shown. The latter has been calculated from the difference between the peak and pretreatment values. Statistics by ANOVA comparing each mean pretreatment value with the respective peak value (*$P < 0.05$). The cytosolic Δ Ca^{2+} of the IL-6 (or IL-11) pretreated groups were similarly compared with Ni^{2+} alone: ‡P = 0.22, §P = 0.75, ‖P = 0.53, ¶P = 0.035, and **P = 0.001.

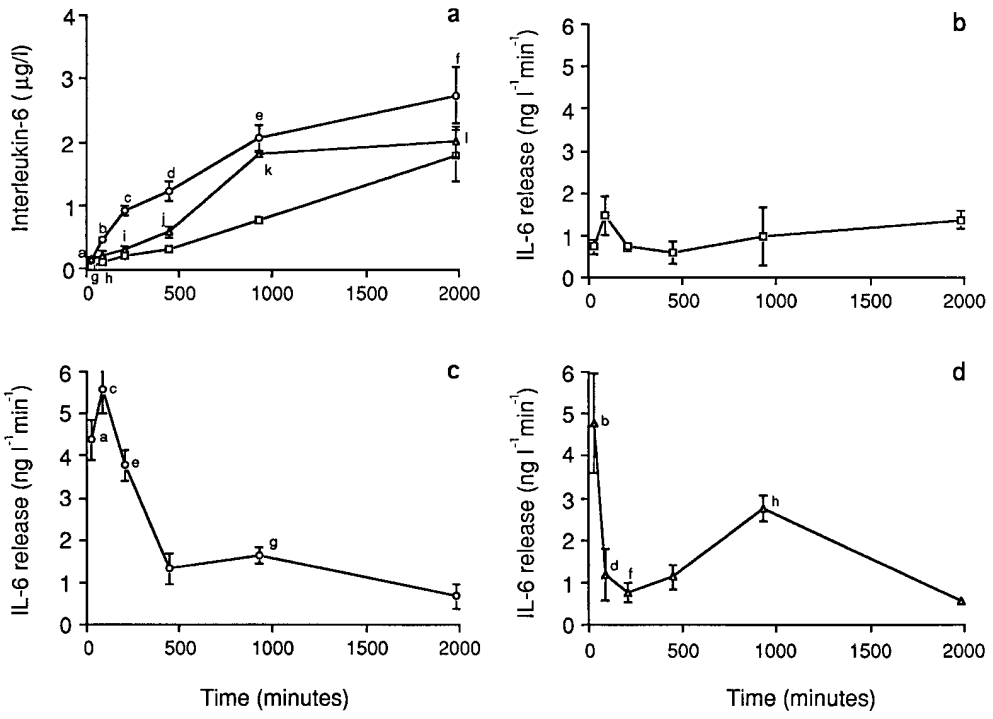

Figure 5. (*a*) Cumulative supernatant levels of IL-6 (μg/l) after incubation of disaggregated osteoclast cultures with either 1.25 mM Ca^{2+} (*squares*) or 10 mM Ca^{2+} (*circles*) (on glass coverslips) or on bone slices (Ca^{2+} = 1.25 mM) (*triangles*). Statistics by ANOVA and Bonferroni's correction for inequality: $^{a,b,c}P = 0.001$, $^{d}P = 0.05$, $^{e}P = 0.0021$, $^{f}P = 0.47$, $^{g}P = 0.05$, $^{h}P = 0.217$, $^{i}P = 0.13$, $^{j}P = 0.064$, $^{k}P = 0.005$, and $^{l}P = 0.683$, all compared with the corresponding time points for the 1.25 mM Ca^{2+} (on glass) variable. (*b–d*) IL-6 release rates (ng l^{-1} min^{-1}) after incubation of disaggregated osteoclast cultures with either 1.25 mM Ca^{2+} (*b*, *squares*) or 10 mM Ca^{2+} (*c*, *circles*) (on glass coverslips) or on bone slices (Ca^{2+} = 1.25 mM) (*d*, *triangles*). Statistics by ANOVA and Bonferroni's correction for inequality: $^{a}P = 0.05$, $^{b}P = 0.028$, $^{c}P = 0.006$, $^{d}P = 0.740$, $^{e}P = 0.001$, $^{f}P = 0.849$, $^{g}P = 0.087$, and $^{h}P = 0.092$. Note that other contaminating cells in our cultures may contribute to the measured IL-6.

mulative IL-6 concentration steadily increased to >20-fold above basal at 33 h. Mean levels for the three treatment variables, at each time point, followed the rank order 10 mM Ca^{2+} on glass > 1.25 mM Ca^{2+} on bone > 1.25 mM Ca^{2+} on glass (control). ANOVA revealed that the mean IL-6 concentration for the 10 mM Ca^{2+} on glass preparation was significantly higher (*P* values, legend to Fig. 5) than that for the control preparation at all time points up to 930 min. The 1.25 mM Ca^{2+} on bone preparation differed from control only at 30 min (143 ± 36 vs. 21.8 ± 5.52 ng/l; $P = 0.05$) and 930 min (1815 ± 45.7 vs. 763 ± 61.5 ng/l; $P = 0.005$). At 33 h, none of the variables were significantly different from each other.

IL-6 release rate was calculated as the concentration per unit time. Fig. 5 *b* shows that this was almost constant over the 33 h for the 1.25 mM Ca^{2+} on glass preparation (control). With the 10 mM Ca^{2+} on glass treatment variable, there was an initial, highly significant, greater than fivefold rise in IL-6 release within 30 min; the calculated rate then fell to basal within 450 min, at which point the release rate was not significantly different from control (Fig. 5 *c*). In contrast, for the 1.25 mM Ca^{2+} on bone, the release rate showed a similar rise to approximately fivefold within 30 min, fell sharply within 90 min to near-control levels, but then displayed a secondary rise at 930 min. At 33 h, the release rate again fell to a level not significantly different from control (Fig. 5 *d*).

Effect of Ca^{2+} on IL-6 and IL-6R mRNA Levels in Single Osteoclasts

The fact that IL-6 secretion from mature osteoclasts appeared to be Ca^{2+} sensitive prompted us to examine the effects of extracellular Ca^{2+} on IL-6 and IL-6R gene expression in single osteoclasts. Messenger RNA for IL-6, IL-6R, and GA3PD genes was detected by identifying the purple-brown cytoplasmic staining (see Materials and Methods). The cells remained colorless when RT-PCR was performed without added primer (Fig. 6, *Control*). Typically, IL-6 mRNA staining was enhanced in cells preincubated with high Ca^{2+}. The mean CSI (see Materials and Methods) for osteoclasts incubated in 10 or 20 mM Ca^{2+} (mean ± SEM, arbitary units, 58.6 ± 7.68 and 66.1 ± 8.58, respectively) was significantly ($P < 0.001$ for both cases, $n = 10$) higher than that of cells incubated in 1.25 mM Ca^{2+} (27.3 ± 1.81). Additionally, a frequency histogram showed that the control osteoclast CSIs were significantly skewed to the left compared with the CSIs of cells incubated in 10 mM Ca^{2+} (Fig. 7 *a*). The stimulatory effect of Ca^{2+} on IL-6 gene expression thus appeared consistent with the cation's effect on IL-6 secretion.

Similar results were obtained with the IL-6R gene. The mean CSI at 5 and 10 mM Ca^{2+} (18.1 ± 1.42 and 18.6 ± 1.74, respectively) were significantly ($P < 0.001$ for both cases, n = 6–21) elevated compared with 1.25 mM Ca^{2+} (8.32 ± 0.43). However, there was a significant decline in mean CSI at 20 mM Ca^{2+} (10.0 ± 1.66, $n = 6$), so that it was not significantly different from that in 1.25 mM Ca^{2+} ($P = 0.18$). Furthermore, intensely stained osteoclasts predominated in the frequency plot in the 5 mM Ca^{2+} group compared with the 1.25 mM Ca^{2+} group (Fig. 7 *b*). Taken together, the results suggest that extracellular Ca^{2+} not only enhanced the synthesis and secretion of IL-6 but also enhanced the synthesis of its receptor.

Finally, as high Ca^{2+} levels may induce osteoclastic shape changes that could, in turn, introduce artifacts in our

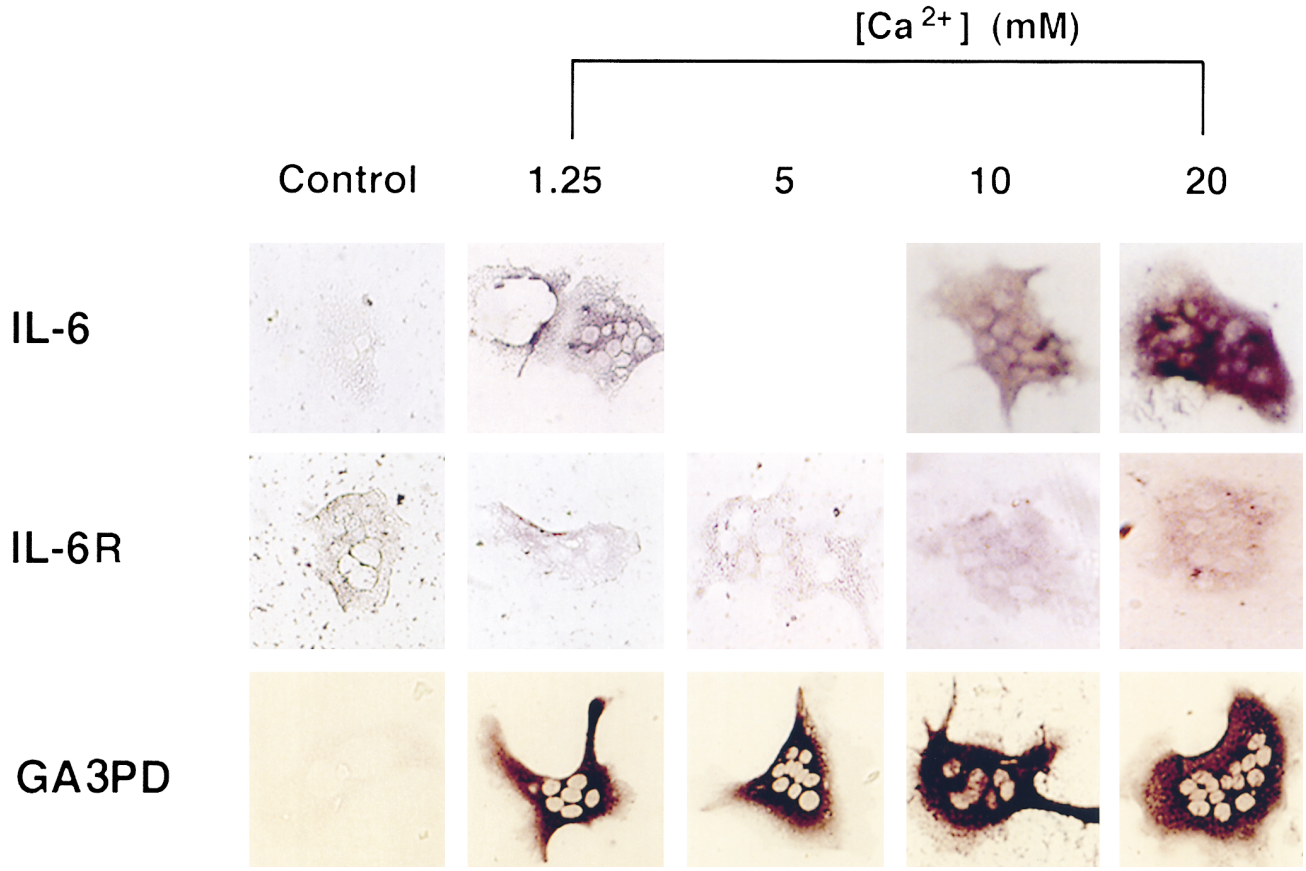

Figure 6. Histostained osteoclasts after in situ RT-PCR for detection of either IL-6 mRNA, IL-6R receptor mRNA, or GA3PD mRNA. The left panels represent controls, i.e., without added primer. For details and primer sequences, refer to Materials and Methods.

densitometric staining evaluation, we studied the expression of the housekeeping gene, GA3PD. We expected its expression to be invariant regardless of whether the extracellular Ca^{2+} levels were high or low. This was indeed the case, suggesting that even subtle shape changes were unlikely to affect our densitometry results to any significant extent.

Discussion

Microelectrode studies have revealed that during each episode of bone resorption, the Ca^{2+} concentration within a resorptive hemivacuole rises to between 8 and 40 mM (Silver et al., 1988). In vitro experiments have demonstrated that such high extracellular Ca^{2+} levels inhibit osteoclastic resorption (for review see Zaidi et al., 1993*b*). Notably, a change in the cell's ambient Ca^{2+} level is sensed by a surface membrane Ca^{2+} receptor (Zaidi et al., 1995). Several morphological and biochemical changes ensue, including reductions in cell attachment, spreading, enzyme release, and acid secretion (Malgaroli et al., 1989; Moonga et al., 1990; Zaidi et al., 1993*b*). We believe that these inhibitory responses to high Ca^{2+} are mediated through Ca^{2+} influx via a surface ryanodine receptor (Zaidi et al., 1993*a*, 1995). Should these changes persist, however, bone resorption would be self-limiting. It is of paramount physiological importance, therefore, to have in place a mechanism for re-establishing resorption after its inhibition by resorbed Ca^{2+}.

It is evident from our study that IL-6, by interacting with its receptor, reverses the inhibitory effect of Ca^{2+} on bone resorption. This reversal correlates with the attenuation, by IL-6, of (*a*) the primary cation-induced Ca^{2+} release response at 0.5 μg/l and above, and (*b*) the secondary, more prolonged, Ca^{2+} influx response at a lower concentration of 5 ng/l. Indeed, Ca^{2+}-induced resorption inhibition is reversed at 5 ng/l IL-6. Furthermore, the secondary phase, as opposed to the primary response, is thought to mediate the long-term effects of Ca^{2+} on resorption (Zaidi et al., 1989). Thus, attenuation of the secondary rise in cytosolic Ca^{2+} by IL-6 may contribute, in part, to the reversal of the antiresorptive effect of Ca^{2+} over the 24-h incubation. Nevertheless, alternate signaling pathways may also be used by IL-6.

It is of note that the closely related cytokine, IL-11, does not mimic the IL-6 effect, although IL-11 receptors apparently exist on osteoclast-like cells (Bellido et al., 1996). This important difference, which establishes the specificity of IL-6 action, is even more striking because the two cytokines, IL-6 and IL-11, share a common transduction pathway. Their distinct α receptor subunits heterodimerize with a common glycoprotein, gp130, to activate several kinases, including the JAK/STAT and MAPK pathways (Hilton et al., 1994; Bellido et al., 1996). It is not known,

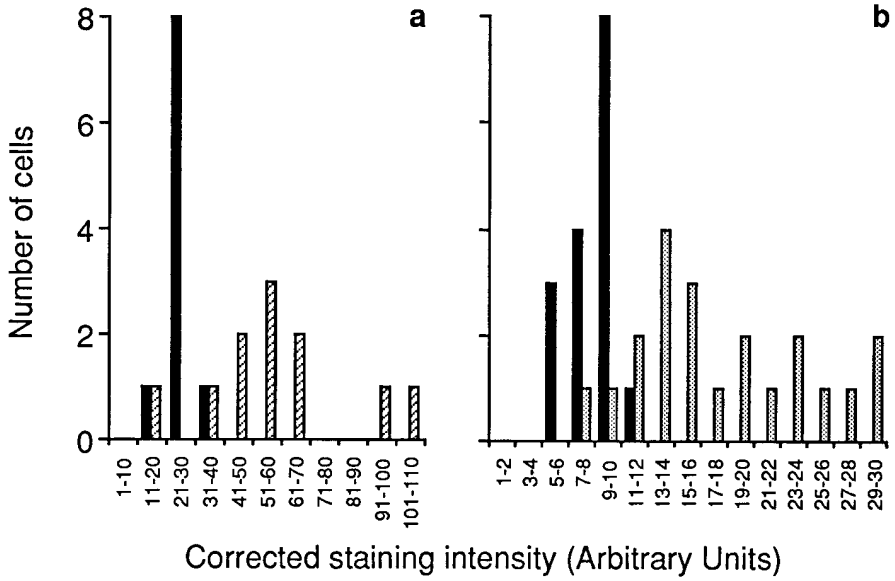

Figure 7. Semiquantitative representation in frequency histograms of corrected staining intensity after in situ RT-PCR for IL-6 mRNA (*a*) or IL-6R mRNA (*b*) for osteoclasts incubated with 1.25 mM Ca^{2+} (*solid black bars*), 5 mM Ca^{2+} (*dotted bars*), or 10 mM Ca^{2+} (*diagonal bars*).

however, which kinase pathway is used by IL-6 to antagonize the Ca^{2+}-induced resorption inhibition. However, as IL-6 abrogates both Ca^{2+} influx and Ca^{2+} release, we suggest that the cytokine acts proximally. As with calcitonin (Zaidi et al., 1996), the Ca^{2+} receptor could itself become inactivated via IL-6–induced phosphorylation.

We next examined whether extracellular Ca^{2+} modulates IL-6 expression in, and secretion from, the osteoclast. Immunoreactive IL-6 levels in control cultures increased to ~20-fold above basal during the 33-h incubation, indicating constitutive IL-6 expression. Furthermore, a rapid induction in IL-6 secretion followed the elevation of extracellular Ca^{2+} from 1.25 mM to 10 mM. In contrast, when osteoclasts were resorbing bone, a rapidly rising phase of IL-6 secretion was followed by a more delayed elevation around 7.5 and 15.5 h. The enhanced secretion of preformed IL-6 could conceivably explain the initial elevations of IL-6. An effect of Ca^{2+} on IL-6 gene transcription nevertheless remains a plausible explanation. It should be noted, however, that other contaminating cells in our cultures might contribute to the measured IL-6.

Finally, we investigated the effect of Ca^{2+} on IL-6 gene expression by incubating osteoclasts for 6 h in the presence of elevated Ca^{2+} levels (5, 10, and 20 mM). A marked enhancement of IL-6 mRNA expression was noted in cells incubated with 10 and 20 mM Ca^{2+} compared with those incubated with 1.25 mM Ca^{2+}. These results may have been confounded by the subtle changes in osteoclast shape induced upon Ca^{2+} exposure that may have affected densitometric staining measurements. However, we found that the expression of a housekeeping gene, GA3PD, did not change under the same experimental conditions. Nonetheless, these results should be treated with caution because of the inherent variability of in situ PCR methodology as well as the densitometric methods used for quantitation.

Although the effect of Ca^{2+} on IL-6 secretion and synthesis appears dramatic, its mechanism remains poorly understood. It is known that Ca^{2+} can regulate transcription of the IL-6 gene promoter (Franchimont et al., 1997). However, it still remains unclear whether Ca^{2+} interacts directly with a Ca^{2+}-response element on the promoter, or whether it acts indirectly via protein kinase C (Shen et al., 1988; Rosen et al., 1995). Furthermore, it is interesting that IL-6R mRNA is elevated in osteoclasts incubated in high Ca^{2+}. Indeed, that the synthesis of a cytokine and its receptor should rise in parallel makes good physiological sense.

Although our results appear to be relevant physiologically, we have no information on the concentration of IL-6 released in situ. The cumulative levels of IL-6 in our cultures, however, do match those required for attenuating Ca^{2+} (cation) sensing and for reversing Ca^{2+}-induced resorption inhibition. It is a paradox then that exogenous but not endogenous IL-6 abrogates the effect of a high Ca^{2+} level. However, in our in vitro pit assay, osteoclasts are exposed to Ca^{2+} during the early phases of resorption and thus become inhibited well before the enhanced IL-6 synthesis and release results in IL-6 accumulation. Furthermore, high extracellular Ca^{2+} will enhance IL-6 secretion only until IL-6 levels rise high enough to inhibit Ca^{2+} sensing. In experiments wherein IL-6 is added together with Ca^{2+}, it is expected that IL-6 would reverse any acute inhibitory effects of the cation, presumably from the initiation of even the first resorptive episode. In addition, IL-6 is known to enhance the transcription of its own gene and, at least hypothetically, this should lead to higher cumulative IL-6 levels.

In conclusion, it is conceivable that the Ca^{2+} generated during normal resorption, which would otherwise inhibit osteoclast activity, enhances IL-6 and IL-6R expression. The secreted IL-6 should then, through a negative autocrine loop, attenuate Ca^{2+} sensing, and hence sustain bone resorption even in the face of a rising Ca^{2+} level. Note, however, that a simple decrease in lacunar Ca^{2+} resulting from diffusion due to cell deadhesion and retraction would also release an osteoclast from Ca^{2+}-induced inhibition.

The authors are grateful to Iain MacIntyre (William Harvey Research Institute, London, UK) and Stavros Manolagas (University of Arkansas for Medical Sciences, Little Rock, AR) for their encouragement and support; Qinwu Lin (Wistar Institute, Philadelphia, PA) for assistance with confo-

cal microscopy; Jerry Rosenzweig and Christine Jones (Geriatrics Department, Philadelphia VA Medical Center, Philadelphia, PA) for assistance; and Rabina Smith and David Douglas (Medical Media, Philadelphia VA Medical Center, Philadelphia, PA) for illustrations.

M. Zaidi acknowledges the support of the National Institutes of Health (RO1-AG14917-02), the Department of Veteran's Affairs, Amgen Pharmaceuticals Inc. (Thousand Oaks, CA), and Merck and Co. (Whitehouse Station, NJ).

Received for publication 19 November 1997 and in revised form 29 July 1998.

References

Adebanjo, O.A., M. Pazianas, A. Zaidi, V.S. Shankar, Z.A. Bascal, C.G. Dacke, C.L.-H. Huang, and M. Zaidi. 1994. Quantitative studies on the effect of prostacyclin on freshly isolated rat osteoclasts in culture. *J. Endocrinol.* 143:375–381.

Bellido, T., N. Stahl, T.J. Farruggella, V. Borba, G.D. Yancopoulos, and S.C. Manolagas. 1996. Detection of receptors for interleukin-6, interleukin-11, leukemia inhibitory factor, oncostatin M, and ciliary neurotropic factor in bone marrow stroma/osteoblastic cells. *J. Clin. Invest.* 97:431–437.

Bellido, T., V.Z. Borba, P. Robertson, and S.C. Manolagas. 1997. Activation of the Janus/STAT (signal transducer and activator of transcription) signal transduction pathway by interleukin-6-type cytokines promotes osteoblast differentiation. *Endocrinology.* 138:3666–3676.

Boyde, A., N.N. Ali, and S.J. Jones. 1984. Resorption of dentine by isolated osteoclasts *in vitro*. *Br. Dental J.* 156:216–220.

Caputo, C. 1981. Nickel substitution for calcium and the timecourse of potassium conductances of single muscle fibres. *J. Muscle Res. Cell Motil.* 2:167–182.

Chambers, T.J., O.A. Revell, K. Fuller, and N.A. Athanasou. 1984. Resorption of bone by isolated rabbit osteoclasts. *J. Cell Sci.* 66:383–399.

Delvin, R.D., H.G. Bone, and G.D. Roodman. 1996. IL-6: a potential mediator of the massive osteolysis in patients with Gorham-Stout disease. *J. Clin. Endocrinol. Metab.* 81:1893–1897.

Dempster, D.W., R.J. Murrills, W.R. Horbert, and T.R. Arnett. 1987. Biological activity of chicken calcitonin: effects on neonatal rat and embryonic chick osteoclasts. *J. Bone Miner. Res.* 2:443–448.

Franchimont, N., S. Rydziel, and E. Canalis. 1997. Interleukin-6 is autoregulated by transcriptional mechanisms in cultures of rat osteoblastic cells. *J. Clin. Invest.* 100:1797–1803.

Greenfield, E.M., M.C. Horowitz, and S.A. Lavish. 1996. Stimulation by parathyroid hormone of interleukin-6 and leukemia inhibitory factor expression in osteoblasts is an immediate-early gene response induced by cAMP signal transduction. *J. Biol. Chem.* 271:10984–10989.

Hilton, D.J., A.A. Hilton, A. Raiceric, S. Rakar, M. Harrison-Smith, N.M. Gough, C.G. Begley, D. Metcalf, N.A. Nicola, and T.A. Wilson. 1994. Cloning of murine IL-11 receptor α chain requirement for gp130 for high affinity binding and signal transduction. *EMBO (Eur. Mol. Biol. Organ.) J.* 13:4765–4775.

Hirata, Y., T. Taga, M. Hibi, N. Nakano, T. Hirano, and T. Kishimoto. 1989. Characterization of IL-6 receptor expression by monoclonal and polyclonal antibodies. *J. Immunol.* 143:2900–2906.

Hughes, D.E., R.L. Jilka, S.C. Manolagas, S. Dallas, L.F. Bonewald, G.R. Mundy, and B.F Boyce. 1995. Sex steroids promote osteoclast apoptosis *in vitro* and *in vivo*. *J. Bone Miner. Res.* 10(Suppl.):48.

Ishimi, Y., C. Miyaura, C.H. Jin, T. Akatsu, E. Abe, Y. Nakamura, A. Yamaguchi, S. Yoshiki, T. Matsuda, T. Hirano, et al. 1990. IL-6 is produced by osteoblasts and induces bone resorption. *J. Immunol.* 145:3297–3303.

Jilka, R.L., G. Hangoc, G. Girasole, G. Passeri, D.C. Williams, J.S. Abrams, B. Boyce, H. Broxmeyer, and S.C. Manolagas. 1992. Increased osteoclast development after estrogen loss: mediation by IL-6. *Science.* 257:88–91.

Kurebayashi, S., Y. Miyashita, T. Hirose, S. Kasayami, S. Akira, and T. Kishimoto. 1997. Characterization of mechanisms of IL-6 gene repression by estrogen receptor. *J. Steroid Biochem. Mol. Biol.* 60:11–17.

Lin, S.-C., T. Yamate, V.Z.C. Borba, G. Girasole, C.A. O'Brien, T. Bellido, E. Abe, and S.C. Manolagas. 1997. Regulation of the gp80 and gp130 subunits of the IL-6 receptor by sex steroids in the murine bone marrow. *J. Clin. Invest.* 100:1980–1990.

MacIntyre, I., M. Zaidi, A.S.M.T. Alam, H.K. Datta, B.S. Moonga, P.K. Lidbury, M.R. Hecker, and J.R. Vane. 1991. Osteoclast inhibition: an action of nitric oxide not mediated by cyclic GMP. *Proc. Natl. Acad. Sci. USA.* 88: 2936–2940.

Malgaroli, A., J. Meldolesi, A. Zabonin-Zallone, and A. Teti. 1989. Control of cytosolic free calcium in rat and chicken osteoclasts. *J. Biol. Chem.* 264: 14342–14347.

Manolagas, S.C., and R.L. Jilka. 1995. Bone marrow, cytokines and bone remodelling. *N. Engl. J. Med.* 332:305–311.

May, L.T., R. Neta, L.L. Moldawer, J.S. Kenney, K. Patel, and P.B. Sehgal. 1993. Antibodies chaperone circulating IL-6 "neutralizing" antibodies in vivo. *J. Immunol.* 151:3225–3236.

Moonga, B.S., D.W. Moss, A. Patchell, and M. Zaidi. 1990. Intracellular regulation of enzyme secretion from rat osteoclasts and evidence for a functional role in bone resorption. *J. Physiol. (Lond.).* 42:29–45.

Moonga, B.S., H.K. Datta, P.J.R. Bevis, C.L.-H. Huang, I. MacIntyre, and M. Zaidi. 1991. Correlates of osteoclast function in the presence of perchlorate ions in the rat. *Exp. Physiol.* 76:923–933.

Narazaki, M., K. Yasukawa, T. Saito, Y. Ohsugi, H. Fukui, Y. Koishihara, G.D. Yancopoulos, T. Taga, and T. Kishimoto. 1993. Soluble form of the interleukin-6 signal-transducing receptor component gp130 in human serum possessing a potential to inhibit signals through membrane-anchored gp130. *Blood.* 82:1120–1126.

Ohsaki, Y., S. Takahashi, T. Scarcez, A. Demulder, T. Nishihara, R. Williams, and G.D. Roodman. 1992. Evidence for an autocrine/paracrine role for IL-6 in bone resorption by giant cells from giant cell tumour of bone. *Endocrinology.* 131:2229–2234.

Roodman, G.D., N. Kurihara, Y. Ohsaki, T. Kukita, D. Hosking, A. Demulder, and F.R Singer. 1992. IL-6 and potential autocrine/paracrine factor in Paget's disease of bone. *J. Clin. Invest.* 8:46–52.

Rosen, L.B., D.D. Ginty, and M.E. Greenberg. 1995. Calcium regulation of gene expression. *In* Advances in Second Messenger and Phosphoprotein Research Vol. 30. A.R. Means, editor. Raven Press, New York. 225–253.

Shankar, V.S., C.M.R. Bax, B.E. Bax, A.S.M.T. Alam, B. Simon, M. Pazianas, B.S. Moonga, C.L.-H. Huang, and M. Zaidi. 1992. Activation of the Ca^{2+} "receptor" on the osteoclast by Ni^{2+} elicits cytosolic Ca^{2+} signals: evidence for receptor activation and inactivation, intracellular Ca^{2+} redistribution and divalent cation modulation. *J. Cell. Physiol.* 155:120–129.

Shen, M., S.T. Dougan, G. McFadden, and M.E. Greenberg. 1988. Calcium and growth factor pathways of c-*fos* transcriptional activation require distinct upstream regulatory sequences. *Mol. Cell. Biol.* 8:2787–2796.

Silver, I.A., R.J. Murrills, and D.J. Etherington. 1988. Microelectrode studies on acid microenvironment beneath adherent macrophages and osteoclasts. *Exp. Cell. Res.* 175:266–276.

Taga, T., M. Hibi, Y. Yamasaki, K. Yasukawa, T. Matsuda, T. Hirano, and T. Kishimoto. 1989. Interleukin-6 triggers the association of its receptor with a possible signal transducer, gp 130. *Cell.* 58:573–581.

Tamura, T., N. Udagawa, N. Takahashi, C. Miyauri, S. Tanaka, Y. Yamada, Y. Koishihara, Y. Ohsugi, K. Kumaki, T. Taga, et al. 1993. Soluble IL-6 receptor triggers osteoclast formation by IL-6. *Proc. Natl. Acad. Sci. USA.* 90: 11924–11928.

Vink, A., P. Coulie, G. Warnier, J.C. Renauld, M. Stevens, D. Donckers, and J. Van Snick. 1990. Mouse plasmacytoma growth in vivo: enhancement by interleukin-6 (IL-6) and inhibition by antibodies directed against IL-6 or its receptor. *J. Exp. Med.* 172:991–1000.

Zaidi, M., H.K. Datta, A. Patchell, B.S. Moonga, and I. MacIntyre. 1989. "Calcium-activated" intracellular calcium elevation: a novel mechanism of osteoclast regulation. *Biochem. Biophys. Res. Commun.* 163:1461–1465.

Zaidi, M., I. MacIntyre, and H.K. Datta. 1990. Intracellular calcium in the control of osteoclast function. II. Paradoxical elevation of cytosolic free calcium by verapamil. *Biochem. Biophys. Res. Commun.* 167:807–812.

Zaidi, M., A.S.M.T. Alam, V.S. Shankar, Bax, B.E., B.S. Moonga, P.J.R. Bevis, M. Pazianas, and C.L.-H. Huang. 1992. A quantitative description of components of *in vitro* morphometric change in the rat osteoclast model: relationships with cellular function. *Eur. Biophys. J.* 21:349–355.

Zaidi, M., A.S.M.T. Alam, C.L.-H. Huang, M. Pazianas, C.M.R. Bax, B.E. Bax, B.S. Moonga, P.J.R. Bevis, and V.S. Shankar. 1993*a*. Extracellular Ca^{2+} sensing by the osteoclast. *Cell Calcium.* 14:271–277.

Zaidi, M., A.S.M.T. Alam, V.S. Shankar, B.E. Bax, C.M.R. Bax, B.S. Moonga, P.J.R. Bevis, C. Stevens, D.R. Blake, M. Pazianas, and C.L.-H. Huang. 1993*b*. Cellular biology of bone resorption. *Biol. Rev.* 68:197–264.

Zaidi, M., V.S. Shankar, C.M.R. Bax, B.E. Bax, P.J.R. Bevis, M. Pazianas, A.S.M.T. Alam, and C.L.-H. Huang. 1993*c*. Linkage of extracellular and intracellular control of cytosolic Ca^{2+} in rat osteoclasts in the presence of thapsigargin. *J. Bone Miner. Res.* 8:961–967.

Zaidi, M., V.S. Shankar, C.L.-H. Huang, B.R. Rifkin, and M. Pazianas. 1994. Molecular mechanisms of calcitonin action. *J. Endocrine.* 2:459–467.

Zaidi, M., V.S. Shankar, R. Tunwell, O.A. Adebanjo, J. MacKrill, M. Pazianas, D. O'Connell, B.J. Simon, B.R. Rifkin, A.R. Ventikaraman, et al. 1995. A ryanodine receptor-like molecule expressed in the osteoclast plasma membrane functions in extracellular Ca^{2+} sensing. *J. Clin. Invest.* 96:1582–1590.

Zaidi, M., V.S. Shankar, O.A. Adebanjo, F.A. Lai, M. Pazianas, G. Sunavala, A.I. Spielman, and B.R. Rifkin. 1996. Regulation of extracellular Ca^{2+} sensing in rat osteoclasts by femtomolar calcitonin concentrations. *Am. J. Physiol.* 271:F637–F644.

Zipori, D., J. Toledo, and K. Von der Mark. 1985. Phenotypic heterogeneity among stroma cell lines from mouse bone marrow disclosed in their extracellular matrix composition and interaction with normal and leukemic cells. *Blood.* 66:447–455.